

TO STUDY THE ROLE OF STRUCTURAL AND ELECTRICAL PROPERTIES OF ZnO/Cu₂O/ITO CORE-SHELL NANOSTRUCTURE SOLAR CELLS

Saw Shine Ko¹, Thida Win², Than Than Win³ and Yin Maung Maung⁴

Abstract

In this work, Zinc Oxide Core layer films and Cu₂O Shell layers were synthesized by using both Chemical Bath Deposition techniques and Spin Coating Method. X-ray diffraction techniques were used to examine the lattice distortion, dislocation density and position parameters of deposited Core-Shell layers upon Indium Tin Oxide glass substrates. Scanning Electron Microscopy (SEM) study provides morphological of the sample surfaces. The photovoltaic properties of these Core-Shell nanostructure solar cells were investigated by current density-voltage characteristic. The power conversion efficiency (PCE) was influenced by the open-circuit voltage.

Keywords: X-ray diffraction, Scanning Electron Microscopy, Power conversion efficiency, Fill factor

Introduction

Core-Shell Nanostructure Solar Cells

In recent years, the optical properties of metallic Core-Shell nanostructure have received particular attention, since, the Core-Shell nanostructures can obtain many unique properties via the combination of different materials (Muehling O et al., 2009). The development of Core-Shell structured materials on a nanometer scale has been receiving extensive attention (Lee H B, 2006).

The shell can alter the charge, functionality and reactivity of the surface, or improve the stability and dispersive ability of the core material (Jing Z et al, 2003).

It is also believed that optical, catalytic or magnetic functions can be imparted to the core particles by the shell material. In general, the synthesis of core/shell structured thin films has the advantage of obtaining a new composite material having synergetic or complementary characteristics of the

¹, Dr, Assistant Lecturer, Physics Department , University of Yangon

², Physics Department, Mandalay University of Distance Education

³, Physics Department, University of Yangon

composites. Many studies on the synthesis of composites i.e. TiO_2 (Bala H et al, 2007), $\gamma\text{Fe}_2\text{O}_3$ (Chou K. S. et al., 2007) and Ag coated with SiO_2 have been reported. The direct band gap increases with increasing in temperature. Annealing at higher temperature decreases the resistivity of Core-Shell structure (Agbo P.E et al., 2011). The study of semiconductor core-shell nanoparticles (NPs) has attracted increasing scientific and technological interest due to the ability to fine-tune their properties, (Caruso R A et al., 2001;Caruso F et al., 2001;Jiang Z et al., 2003;Sertchook H et al., 2003), the most extensive synthesis were focused on type-I core-shell NPs (Mokari T et al., 2003;Protiere M et al., 2007), in which a wide band gap material is coated onto the core of a narrow band gap material. There have been relatively rare reports concerning the preparation of reverse type I core-shell NPs(Zhong X et al., 2005) in which a narrow band gap material is over grown on the core of a wide band gap material and unique characteristic must be observed. Indium tin oxide, widely used in solar cells and optoelectronic devices,(Liu Q et al., 2005) is a direct wide band gap and photostable (Sirimanne P M et al., 2000) material (~ 3.6 eV) (Levi S A et al., 2001;Kim W T et al., 1986). A type II core-shell that facilitates charge separation, a key step for the formation of the photocurrent, and the large band gap semiconductors (e.g., ZnO and ZnSe), which on their own neither of can be an efficient light absorber, by working together they can absorb a much broad spectrum of light as through the type II core-shell has a much lower band gap than any of the components. Therefore, an array of type II core-shell nanowires in particular, can make an efficient solar cell (Zhang Y et al., 2007).

Experimental procedure

Preparation of ITO/ZnO/Cu₂O core-shell thin film

For the preparation of Cu_2O shell layer deposited onto Zinc oxide core layer, Cuprous oxide and 2-methoxyethanol were chosen as the starting materials. 50g of Cu_2O powder were weighted by digital balance. To reduce the particle size, Cu_2O powder was ground by an agate motor for 5hours. After that, Cu_2O fine powder was applied by ball milling method. The milling interval was set for 6 hours. Sample was milled in a grinding bowl (volume of 50g) and grinding ball (20 balls, 5mm diameter dimension) at 250 rpm in

ambient temperature. To get the uniform and lightest particles, all mesh-sieves are cleaned and assembled them in the ascending order of sieve number (100mesh sieve, 250 mesh sieve and 400 mesh sieve) and sieving with 3 times. After 30 min, it was carefully weight of last sieve with its retained powder. Cuprous oxide Shell layer thin films were prepared by the sol-gel spin coating method. First, the copper precursor solution was prepared using Cu_2O powder, 2-methoxyethanol as the solute, solvent and solution stabilizer respectively. Cuprous oxide (3.5g) was first added in amount of 3ml 2-methoxyethanol solution. After 30 min of stirring with 300 rpm at room temperature the hot plate temperature was ramped up to 60°C to 80°C ranges to obtain a homogenous solution. After the process for preparation sol-solution, all the Cu_2O paste were coated onto the ITO/ZnO substrates at a speed of 3000 rpm 30s and at the end of above process coated films were annealed at 150 °C for 3h placed on the hot plate and provided each of them and finally provided post annealing temperature 300°C and 400 °C at muffle furnaces.

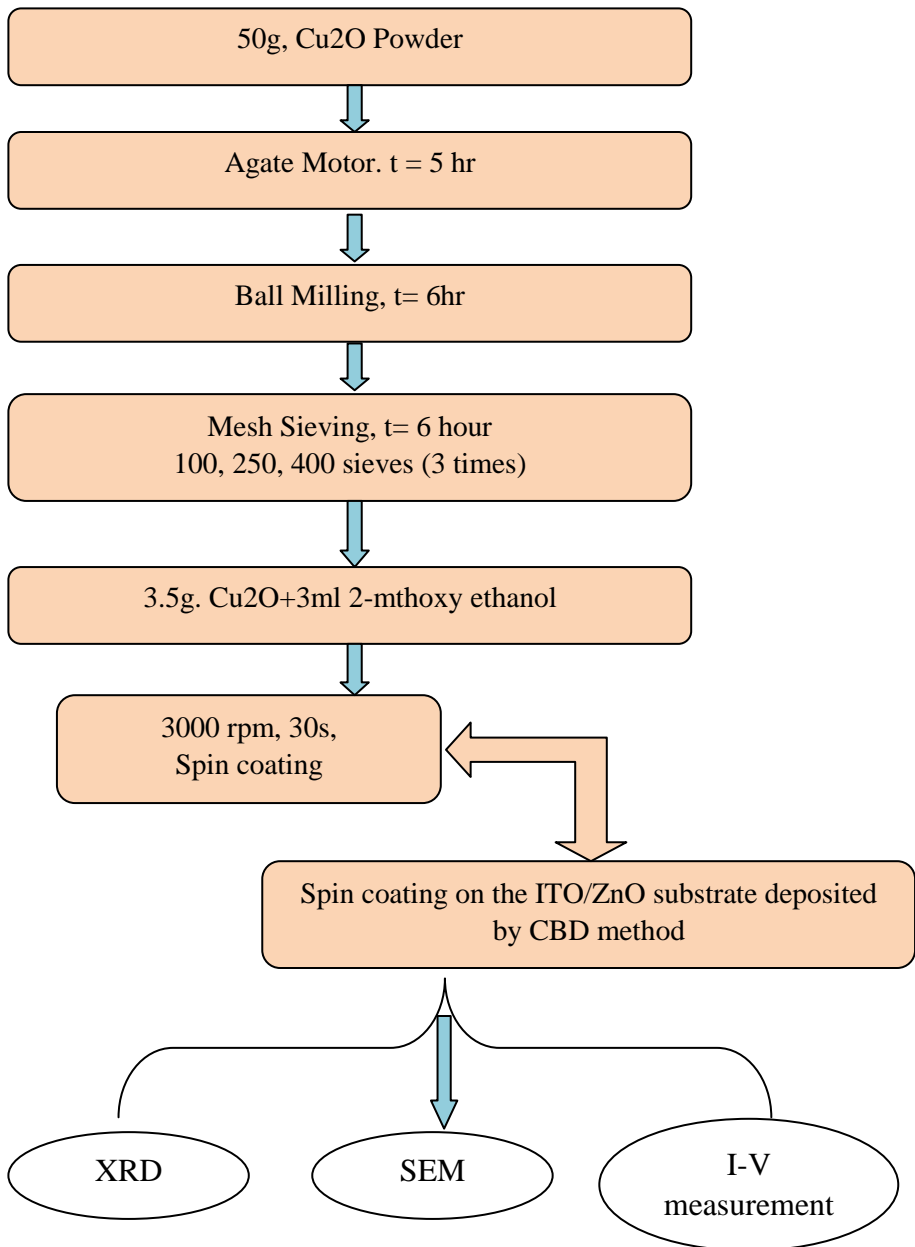


Figure 1.1: Flow chart for preparation of ITO/ZnO/Cu₂O Core-Shell layers deposited with different method on ITO glass substrate with different annealing temperature

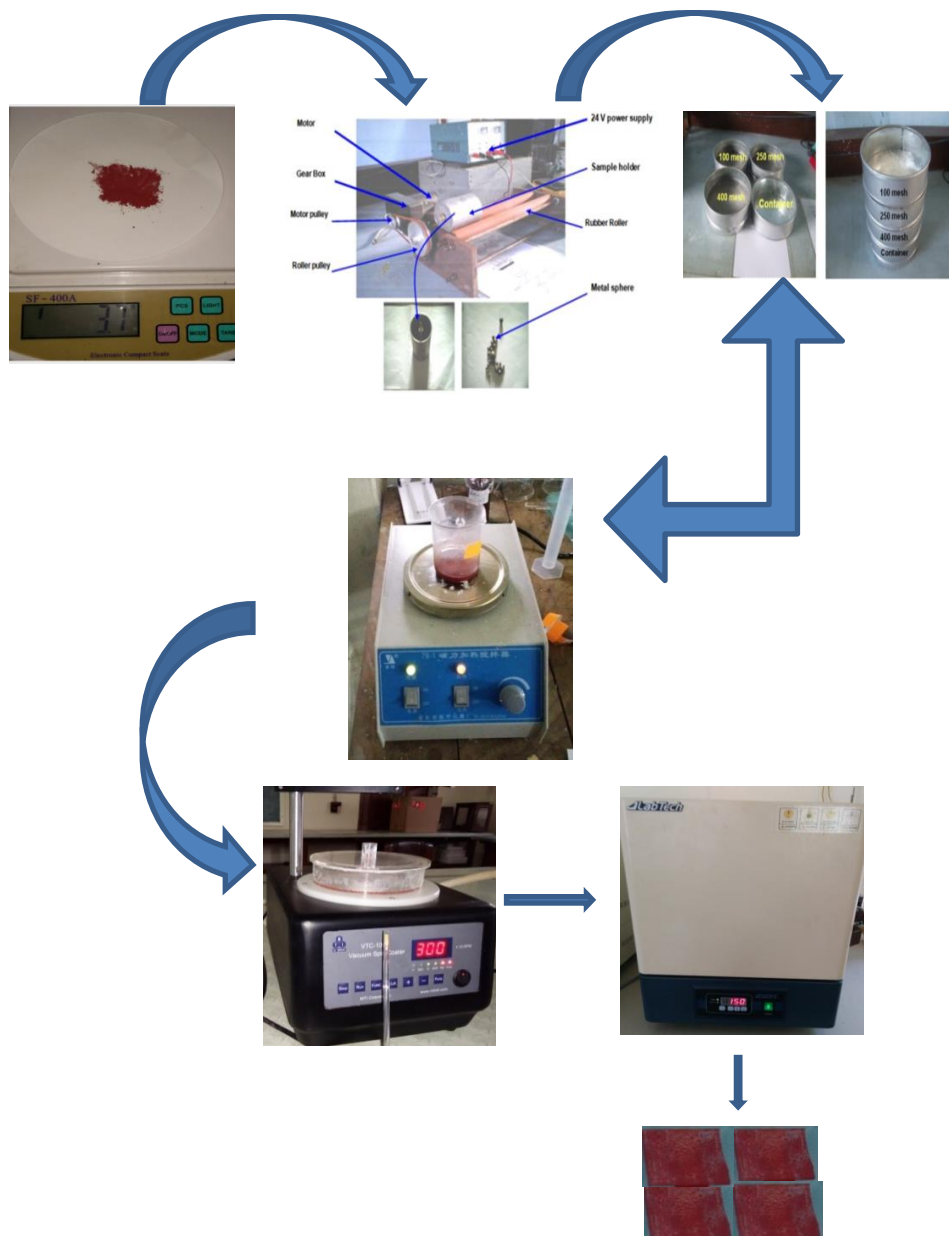


Figure 1.2: The photo depicted to the step by step preparation of Cu_2O Shell thin film onto ZnO/ITO substrate by spin coating technique

Results and Discussion

XRD analysis

X-ray diffraction (XRD) is the most well-known family of techniques to investigate structural properties of a material. Traditionally, XRD is employed on thick or powdered materials because of its penetration depth and thus its ability to reveal internal structural properties are often investigated by surface characterization techniques (e.g., atomic force microscopy), approximating the internal structure as being similar to the surface structure changes have been seen in organic ultra-thin films (Xu Z et al., 2009; Campoy Quiles M et al., 2008; Widjonarko N E et al., 2014; Mauger S A et al., 2013).

$$D = \frac{K \lambda}{\beta_{hkl} \cos \theta} \quad (1)$$

Where β_{hkl} is the integral half width, K is a constant equal to 0.90, λ is the wavelength of the incident X-ray using source of $\text{CuK}\alpha$ ($\lambda = 1.54056 \text{ \AA}$), D is the crystallite size, and θ is the Bragg angle.

Structural analysis of the Cuprous oxide shell layer thin films deposited onto the ITO/ZnO Core thin films annealed at 300°C and 400°C were carried out by using $\text{CuK}\alpha$ radiation source of wavelength ($\lambda = 1.54056 \text{ \AA}$) and the diffraction patterns of films were recorded by varying diffraction angle (2θ) in the range 10° - 70°. From figure (2.1) showed the X-ray diffraction patterns of Cuprous oxide Shell thin layer films deposited on the ITO/ZnO Core thin layers. The X-ray diffraction patterns of Cuprous Oxide thin films elaborated with sample I show high intensity of picks observed peaks matched with characteristic peaks of the Cuprite, Cu_2O (ICDD 01-077-7719) at $2\theta = 36.536^\circ$, 42.424° and 61.620° corresponds to the (1 1 1), (2 0 0) and (2 2 0) diffraction planes and some small peaks assigned to (1 0 0), (0 0 2), (1 0 2), (110), (1 0 3) and (1 1 2) observed at $2\theta = 31.783^\circ$, 34.490° , 47.693° , 56.540° , 63.093° and 68.109° were perfectly matched with the characteristic peaks of Zinc Oxide wurtzite structure, ZnO, (ICDD# 01-075-0576).

At sample II, Figure (2.2) showed the X-ray diffraction patterns of cuprous oxide Shell thin layer films deposited on the ZnO/ITO Core thin layers. The X-ray diffraction patterns of Cuprous Oxide thin films elaborated

with sample II show high intensity of peaks observed peaks matched with characteristic peaks of the Cuprite, Cu_2O (ICDD 01-077-7719) at $2\theta = 36.480^\circ, 42.315^\circ$ and 61.412° corresponds to the (1 1 1), (2 0 0) and (2 2 0) diffraction planes and some small peaks assigned to (1 0 0), (0 0 2), (1 0 2), (1 1 0), (1 0 3) and (1 1 2) observed at $2\theta = 31.871^\circ, 34.575^\circ, 47.750^\circ, 56.777^\circ, 63.139^\circ$ and 68.201° were perfectly matched with the characteristic peaks of Zinc Oxide wurtzite structure, ZnO , (ICDD# 01-075-0576).

The crystallite size of dominant plane (1 1 1) at different annealing temperature were found to be 20.18 nm and 32.25 nm respectively. Improved in crystallinity quality with rising annealing temperature. As a result, oxygen defect are favorable to the merging process to form the larger grains size while increasing the annealing temperature and their treated time. According to the above XRD analysis, the observable peak were good agreement with standard ICDD data reference file (card no 01-077-7719 and 01-075-0576). No unidentifiable peaks were not found in observable spectrum.

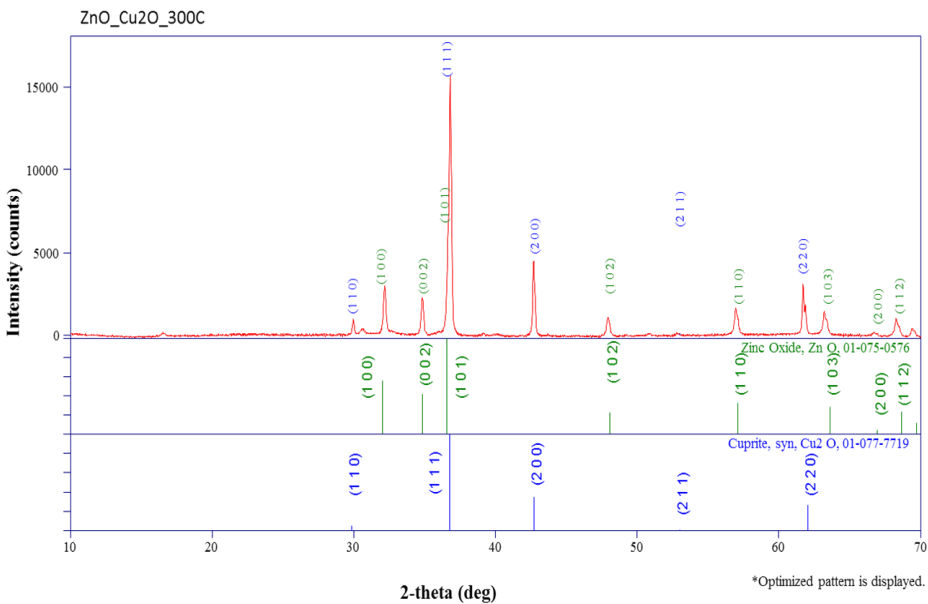


Figure 2.1: X-ray diffraction pattern of ITO/ZnO/Cu₂O Core-Shell thin film annealed at 300°C

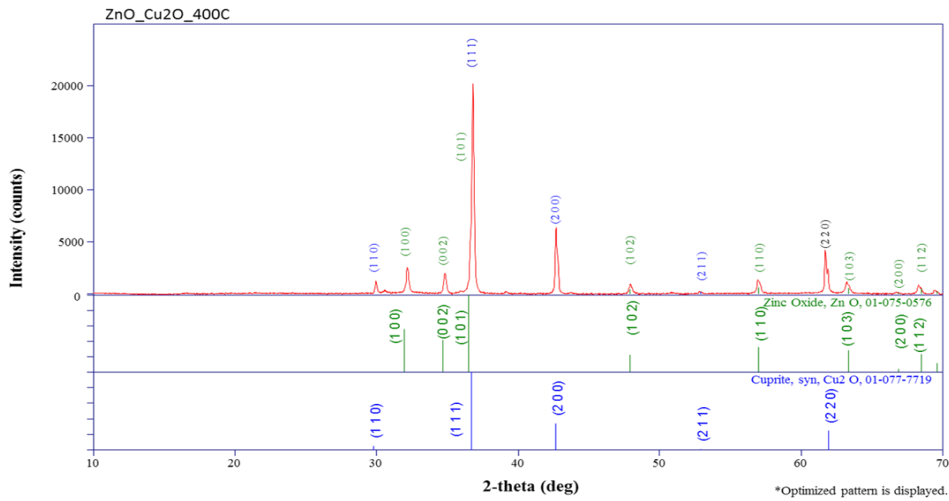


Figure 2.2: X-ray diffraction pattern of ITO/ZnO/Cu₂O Core-Shell thin film annealed at 400°C

Table 1.1: The comparison of Standard 2θ and Observed 2θ value for ITO/ZnO/Cu₂O core-shell thin film annealed at 300°C

(h k l)	Crystal structure	Observed (2θ) (deg)	Standard (2θ) (deg)
(1 0 0)	Hexagonal	31.783	31.941
(0 0 2)	Hexagonal	34.490	34.589
(1 1 1)	Cubic	36.536	36.476
(2 0 0)	Cubic	42.424	42.307
(1 0 2)	Hexagonal	47.693	47.709
(1 1 0)	Hexagonal	56.540	56.770
(2 2 0)	Cubic	61.620	61.374
(1 0 3)	Hexagonal	63.093	63.026
(1 1 2)	Hexagonal	68.109	68.121

Table 1.2: FWHM and Crystallite size value for ITO/ZnO/Cu₂O thin film annealed at 300°C

(h k l)	FWHM (deg)	Crystallite size(nm)
(1 0 0)	0.251	31.61
(0 0 2)	0.292	27.17
(1 1 1)	0.393	20.18
(2 0 0)	0.287	27.64
(1 0 2)	0.588	13.49
(1 1 0)	0.209	37.96
(2 2 0)	0.342	23.20
(1 0 3)	0.643	12.34
(1 1 2)	0.351	22.60

Table 2.1: The comparison of Standard 2θ and Observed 2θ value for ITO/ZnO/Cu₂O thin film annealed at 400°C

(h k l)	Crystal structure	h k l	Observed (2θ) deg	Standard (2θ) deg
(1 0 0)	Hexagonal	(1 0 0)	31.871	31.941
(0 0 2)	Hexagonal	(0 0 2)	34.575	34.589
(1 1 1)	Cubic	(1 1 1)	36.480	36.476
(2 0 0)	Cubic	(2 0 0)	42.315	42.307
(1 0 2)	Hexagonal	(1 0 2)	47.750	47.709
(1 1 0)	Hexagonal	(1 1 0)	56.777	56.770
(2 2 0)	Cubic	(2 2 0)	61.412	61.374
(1 0 3)	Hexagonal	(1 0 3)	63.139	63.026
(1 1 2)	Hexagonal	(1 1 2)	68.201	68.121

Table 2.2: FWHM and Crystallite size value for ITO/ZnO/Cu₂O thin film annealed at 400°C

(h k l)	Observed (d) (Å)	Standard (d) (Å)
(1 0 0)	0.534	14.85
(0 0 2)	0.164	48.38
(1 1 1)	0.246	32.25
(2 0 0)	0.305	26.01
(1 0 2)	0.427	18.58
(1 1 0)	0.630	12.59
(2 2 0)	0.365	21.73
(1 0 3)	0.306	25.93
(1 1 2)	0.295	26.89

SEM analysis

The surface morphology and chemical composition of the ITO/ZnO/Cu₂O Core-Shell thin films were analyzed using a Scanning Electron Microscope coupled with an Energy dispersive X-ray analysis. Bar code size was formed to be 5 μ m with magnification of 15 kV × 4400 and EHT 3.00 kV. Both of the samples consist of randomly distributed grains with a smaller size and shape and with limited porosity. The average grain size of this film for sample I was 1.53 μ m. Fig 3.2 shows that at lower concentration of dopant, the numbers of Cu₂O shell distributed on ZnO core thin layer. The average grain size of 400°C ITO/ZnO/Cu₂O core shell thin film was 1.74 μ m.

Table 3.1: Deposited films, average grain size for ITO/ZnO/Cu₂O Core-Shell films annealed at different temperature.

Annealing temperature	Deposited film	Average Grain Size(μm)
300 °C	ITO/ZnO/Cu ₂ O	1.53
400 °C	ITO/ZnO/Cu ₂ O	1.74

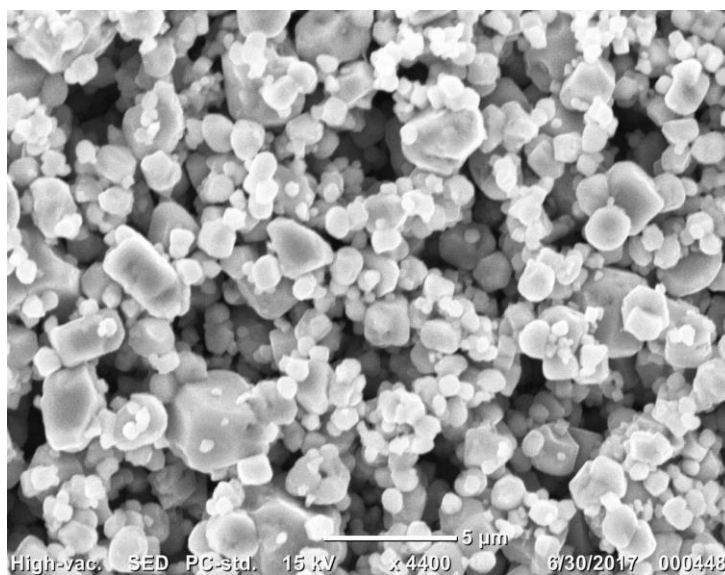


Figure 3.1: SEM analysis image for ITO/ZnO/Cu₂O Core-Shell film annealed at 300°C.

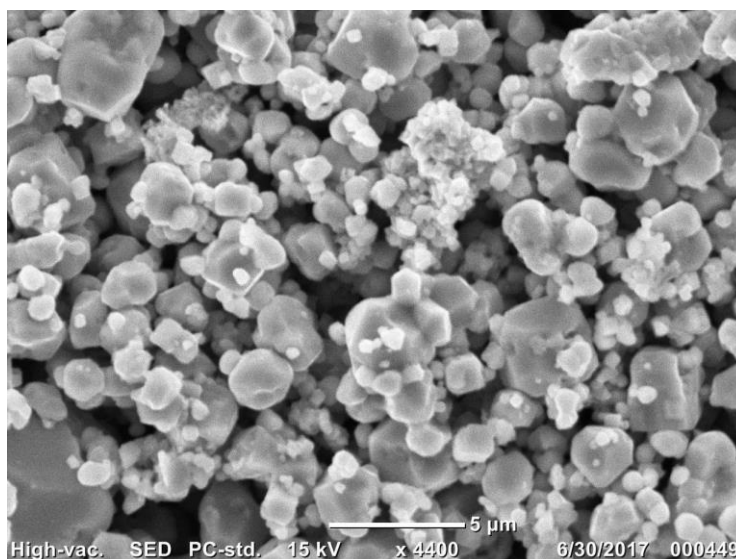


Figure 3.2: X-ray diffraction pattern of ITO/ZnO/Cu₂O Core-Shell film annealed at 400°C

Current - voltage analysis

The current–voltage measurement of the ITO/ZnO/Cu₂O core-shell thin films has been measured at room temperature in the dark and under illumination (Halogen lamp 100W). Dark current-voltage (dark I-V) measurement are commonly used to analyze the electrical characteristic of solar cells, providing an effective way to determine fundamental performance parameters without the need for a solar simulator. I-V characteristics of ITO/ZnO/Cu₂O core-shell thin film are measured in the region of -5V to +5V by using Cu-electrode. Ln I-V characteristics obey the linear relationship and I_s was obtained by extrapolating the variation line in which $I_s = \exp$ (intercept) relation is used. The forward applied voltage ranges, the ideality factor (η), zero bias barrier height (ϕ_{bo}) are measured by the following equation:

$$I_s = A R^* T^2 \exp \frac{-q \phi_{bo}}{kT} \quad \text{-----}(2)$$

$$\frac{1}{n} = \left(1 - \frac{\partial \phi_{bo}}{\partial V_f} \right) \quad \text{-----}(3)$$

I_s = Saturation current

A = diode area

R^* = Richardson constant ($8.16 \text{ A } k^{-2} \text{ cm}^{-2}$)

q = electron charge ($1.6 \times 10^{-19} \text{ C}$)

ϕ_{bo} = Zero biased barrier height

k = Boltzmann constant (1.38×10^{-23}) JK⁻¹

n = Ideality factor

V_f = forward voltage

I-V characteristics of ITO/ZnO/Cu₂O Core-Shell thin layer films at various annealing temperature under illumination condition. These figure demonstrates V_{oc} - I_{sc} characteristics of Core-shell ZnO/Cu₂O/ITO thin layer films at different annealing temperature under illumination condition. Measurement for I-V curves, open circuit voltage (V_{oc}) and short-circuit current (I_{sc}) are carried out using a FLUKE meter, PSN-305_D 30 A Dual voltage source, Lux meter (AS-803) series, and Digital multimeter (UT-120) series. A halogen lamp is used as the source of monochromatic light.

Measurements under illumination with 1000 Lux are performed to estimate the power-conversion efficiency (PCE) and fill factor (FF) of the device under test. It is observed that the value of fill factor for ITO/ZnO/Cu₂O Core-Shell thin layer films annealed at different temperature was 0.80 for ITO/ZnO/Cu₂O Core-Shell thin layer annealed at 300°C and 0.55 for ITO/ZnO/Cu₂O Core-Shell thin layer annealed at 400°C.

The conversion efficiency is the percentage of power converted from absorbed light to electrical energy and collected, when photovoltaic cell is connected to an electrical circuit. The value of the open-circuit voltage, short circuit current, fill factor, and conversion efficiency at various annealing temperature are collect in Table (3.2).

Table 3.1: Ideality factor, Barrier height, and Saturation current density values for ITO/ZnO/Cu₂O core shell nanostructure solar cells at different annealing temperature.

Annealing Temperature(°C)	Ideality factor(n)	Barrier height potential(ϕ_{bo}) eV	Saturation current(μA)
ITO/ZnO/Cu ₂ O300°C	1.48	0.33	8.57×10^{-7}
ITO/ZnO/Cu ₂ O400°C	1.42	0.29	2.91×10^{-7}
[Nadir Habubi F et al., 2015]	1.71	0.69	6.14×10^{-6}

Table 3.2: Photovoltaic measurement for ITO/ZnO/Cu₂O Core-Shell films deposited on ITO thin films under illumination conditions.

Sample	V_{oc} (mV)	I_{sc} (μA)	Fill factor (%)	PCE(%)
ITO/ZnO/Cu ₂ O(300°C)	344.80	7.27	0.80	1.34
ITO/ZnO/Cu ₂ O(400°C)	315.00	13.2	0.55	1.53
FTO/ZnO/CuO/Al(Thowra Abd Elradi Daldowm et al.,2015)	221.00	2.858(mA)	0.99	6.24

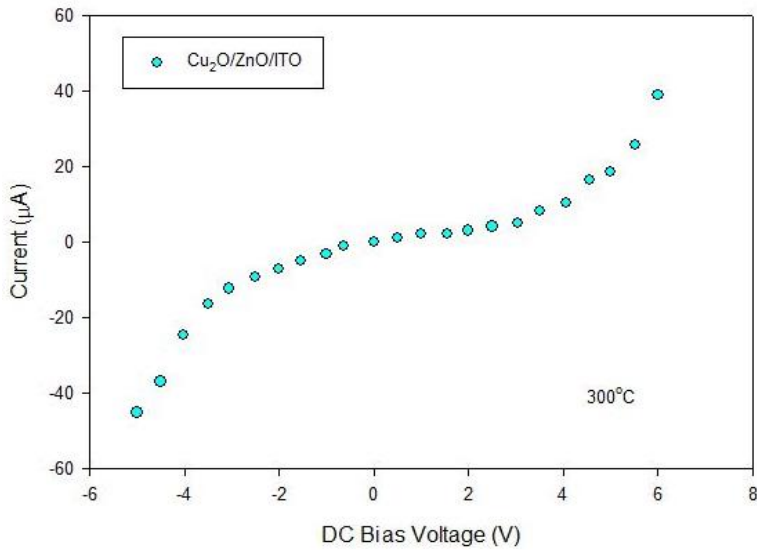


Figure 5: I-V characteristic of dark condition ITO/ZnO/Cu₂O Core-Shell thin film annealed at 300°C

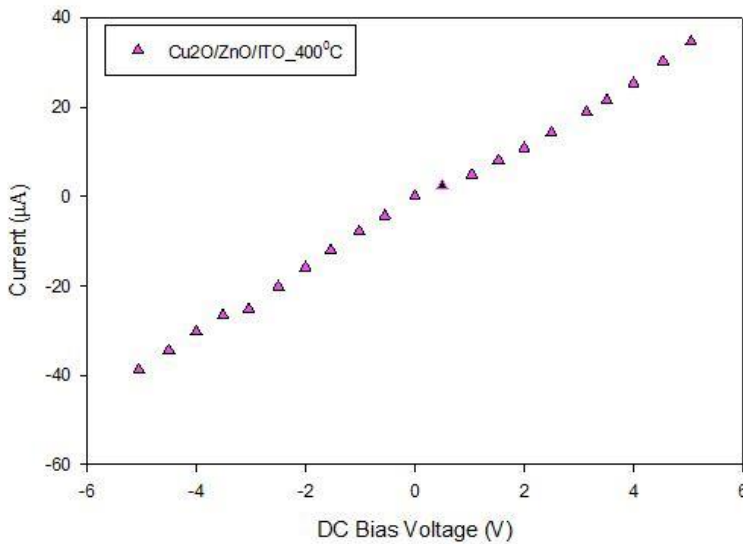


Figure 6: I-V characteristic of dark condition ITO/ZnO/Cu₂O Core-Shell thin film annealed at 400°C

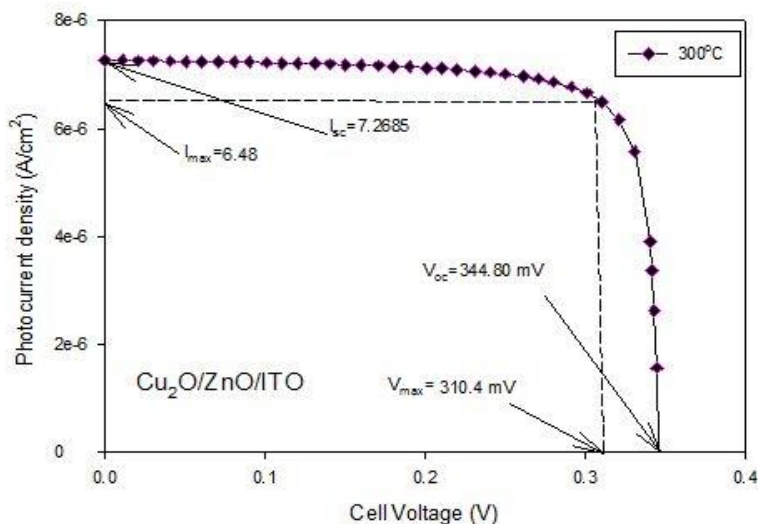


Figure 7: I-V characteristic under illumination condition ITO/ZnO/Cu₂O core shell film annealed at 300°C

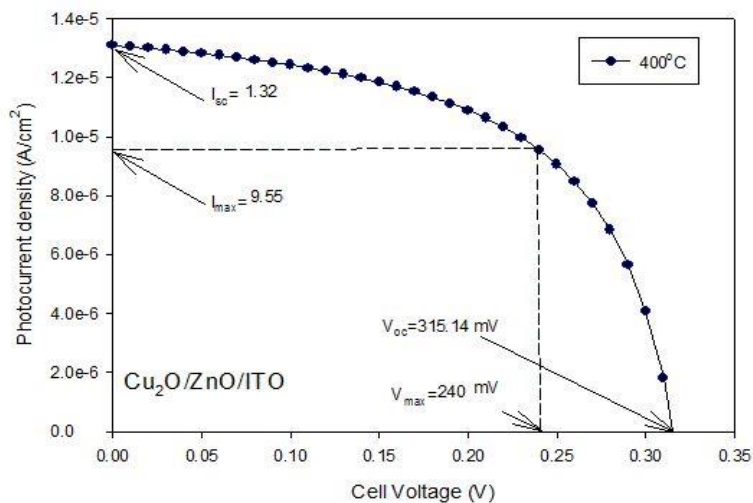


Figure 8: I-V characteristic under illumination condition ITO/ZnO/Cu₂O core shell film annealed at 400°C

Conclusion

In this research, the fabrication and characterization of a device application of ITO/ZnO/Cu₂O core-shell nanostructure solar cells has been investigated. XRD analysis showed that the core-shell thin film is crystallized in the hexagonal phase. The average crystallite size calculated for deposited ITO/ZnO/Cu₂O Core-Shell thin layer films annealed at 300°C and 400 °C were 20.21 nm and 32.28 nm. The electrical parameters such as ideality factor (n) and potential barrier (ϕ_{b0}) are formed to be strongly temperature dependent. The ideality factor of ITO/ZnO/Cu₂O core-shell thin films decreases while the corresponding barrier potential height decreasing with an increasing temperature. The ideality factor is an important parameter for device performance. All the core-shell thin films showed a clear rectifying behavior in the current-voltage characteristic at room temperature. The ideality factor was 1.48-1.42 at the lower voltage region in forward bias. From the I-V measurement under the illumination condition, the value of fill factor for ITO/ZnO/Cu₂O Core-Shell thin layer films annealed at different temperature was 0.80 for ITO/ZnO/Cu₂O Core-Shell thin layer annealed at 300°C and 0.55 for ITO/ZnO/Cu₂O Core-Shell thin layer annealed at 400°C. So, it can be concluded that the fabricated ITO/ZnO/Cu₂O core-shell thin film solar cells is quite suitable for photovoltaic applications.

Acknowledgement

Special thanks to Professor Dr Khin Khin Win, Head of Department of Physics, University of Yangon, for her kind permission.

I am greatly indebted to Professor Dr Aye Aye Thant, Department of Physics, University of Yangon, for her encouragement.

I am also deeply grateful to Dr Yin Maung Maung , Associate Professor , Department of Physics, University of Yangon, for her valuable advice in my experimental work.

Special thanks to Supervisor Dr Thida Win, Lecturer, Department of Physics, University of Yangon, for her valuable advice and supervision throughout in this research.

References

- Avinash Dive S., Deepak., et al,(2015), "Growth structural optical and electrical properties of ZnO thin films Deposited by chemical bath deposition technique", 8,189.
- Basol .B.M., et al,(1985),"Effects of heat treatment on the composition and semiconductivity of electrochemically deposited CdSe films",58,601.
- Cao.B &Cal .W., et al,(2008),"ZnO nanorods to nanoplates chemical bath deposition growth and surface related emission",112,680..
- Danahher W.J., et al,(1978),Nature 271,139.
- Fulop G.F., et al, (1985),"Mater.Sci", 15,197.
- Guozhi Jia,Yunfeng Weng, Jianghong Yao et al.,(2010),"Growth mechanism of ZnO nano-structure using chemical bath deposition",6,303.
- Jhon Harper, Xin-dong Wang., et al.,(2010),"I-V,C-V and AC Impedance Techniques and characterization of Photovoltaic cells",2044.
- Kroger F.A., et al, (1978), "J.Electrochem.Sci", 125, 2082.
- Mandal S.K., et al,(2006), "Thin solid films", 515, 2535.
- Malevu T.D& Ocaya R.O.,et al,(2015),"Effect of Annealing temperature on structural, Morphology and optical properties of ZnO nano-needles prepared by Zinc-Air cell system Method",10,1752.
- Nanda Shaki & Gupta P.S., et al,(2010),"Structural and optical properties of Sol-gel prepared ZnO Thin film",2,19.
- Nadir F.Habubi, Abdulazeez O.Mousa, Noor A, Nema,(2015),"Fabrication and characterization of ZnO/P-Si Heterojunction Solar cell",18,118.
- Ortega .J., et al, (1989), "J Electrochem.Soc", 136, 3388.
- Panicker M.P.R ., et al, (1978), "J.Electrochem .Soc", 125, 568.
- Prabakaran Kandasamy & Amalraj Lourdasamy.,(2014),"Studies on zinc oxide thin films by chemical spray pyrolysis technique",9,261.
- Widjonarko, N.E., et al, (2014), "Impact of hole transport layer surface properties on the morphology of a polymer fullerene bulk heterojunctions," 4, 1301879.
- Wolden, C.A., & Kurtin, J., (2011), "J. Vac. Sci. Technology," 29, 30801.
- White, B., & Yin, M., (2006), "The structural and optical properties of Cu2O films electrodeposited on different substrates," 20,44.

- Xu, H., & Wang, W., (2006), "Shape evolution and size controllable synthesis of Cu₂O octahedral and their morphology dependent photo catalytic properties," 110, 13829.
- Xin Xin Ma & Gang Wang., (2007), "characteristics of copper oxide films deposited by PBII& D," 201, 6712.
- Xu, Z., & Yang, L.M., (2009), "Vertical phase separation in poly (2-hexylthiophene) fullerene derivation blends and its advantages for inverted structure solar cells," 19, 1227-1234.
- Yang, H., & Wang, J., (2011), "Layer structured ZnO nanowire arrays with dominant surface and acceptor related emissions," 65, 1351-1354.
- Zhou, Y.C., & Switzer, J.A., (1998), "Galvan static electrodeposited microstructure of cuprous (I) oxide films," 2,22.
- Zhu, J., & Yu, C. M, (2010), "Nanodome solar cells with efficient light management and self-cleaning nano let," 10, 1979-1984.
- Zaboborski, et al, (2010), "Effect of ionic liquid and surfactants on zinc oxide nanoparticles activity in cross linking of acrylonitrile butadiene elastomers," 116, 155-164.
- Zhang, Y., & Wang, L.W., (2007), "Quantum coaxial cables for solar energy harvesting Nano letters," 7, 1264-1269.